Supplementary Figure 1, Cohen *et al.*

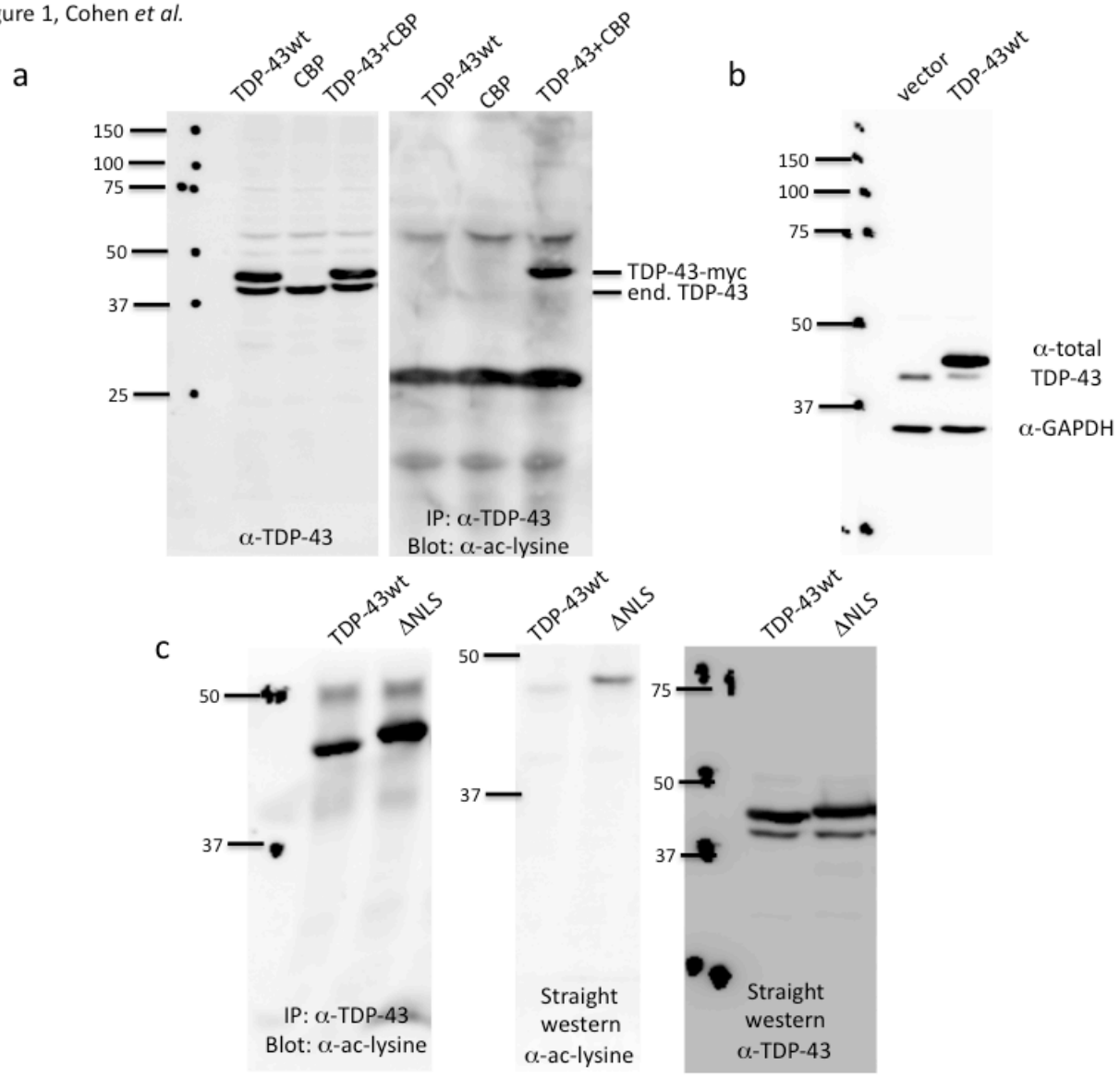

Supplementary Figure 2, Cohen *et al.*

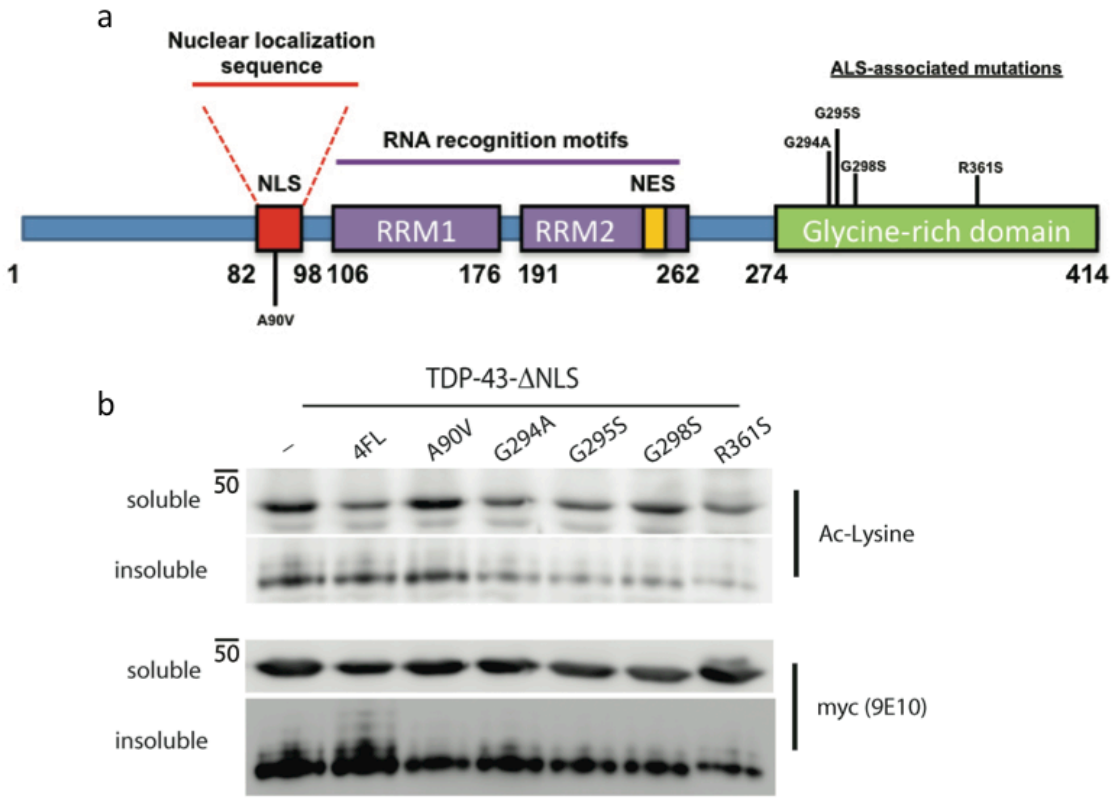

Supplementary Figure 2: TDP-43 acetylation of a panel of ALS-associated TARDBP mutations

a) A schematic of the TDP-43 protein depicting the nuclear localization sequence (NLS), RNA-recognition motifs (RRMs), and C-terminal glycine-rich domain harboring the majority of the ALS-associated genetic mutations. b) Cells were co-transfected with Creb-binding protein (CBP) and the following cytoplasmic targeted expression plasmids: unmodified TDP-43-ΔNLS (positive control for acetylation), TDP-43-ΔNLS containing ALS-associated mutations (A90V, G294A, G295S, G298S, R361S), or TDP-43-ΔNLS containing 4FL RNA-binding deficient mutations in RRM1 and RRM2 (F147/149/229/231L). Cell lysates were evaluated by immunoprecipitation and western analysis using an anti-acetyl-lysine antibody. There were no appreciable differences in TDP-43 acetylation status among the various mutants compared to TDP-43-ΔNLS.

Supplementary Figure 3, Cohen *et al.*

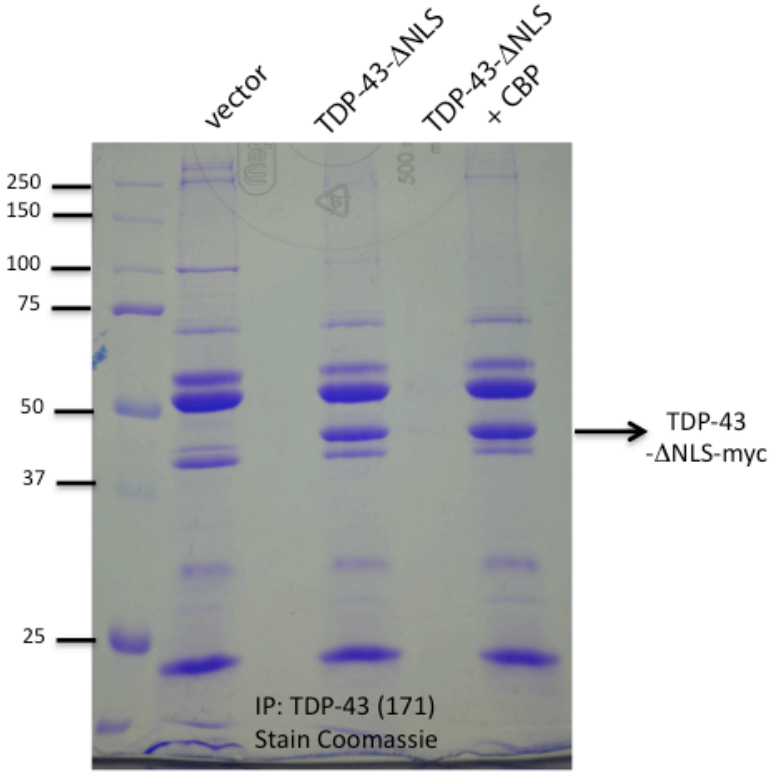

Supplementary Figure 4, Cohen *et al.*

#	b	b-H2O	b-NH3	b (2+)	Seq	y	y-H2O	y-NH3	y (2+)	#
1	102.06	84.04	85.03	51.53	T					11
2	159.08	141.07	142.05	80.04	G	1133.58	1115.72	1116.56	567.29	10
3	296.24	278.12	279.35	148.57	H	1076.92	1058.55	1059.54	538.78	9
4	383.34	365.29	366.38	192.08	S	939.59	921.38	922.48	470.25	8
5	553.39	535.33	536.25	277.14	K(+42.01)	852.61	834.16	835.45	426.74	7
6	610.29	592.28	593.24	305.65	G	682.46	664.02	665.65	341.68	6
7	757.34	739.47	740.34	379.18	F	625.64	607.60	609.00	313.17	5
8	814.30	796.70	796.70	407.69	G	478.36	460.27	461.36	239.64	4
9	961.44	943.48	944.43	481.23	F	421.27	403.25	404.09	211.13	3
10	1060.49	1042.49	1043.49	530.76	V	274.28	256.18	257.21	137.59	2
11					R	175.35	157.11	158.09	88.06	1

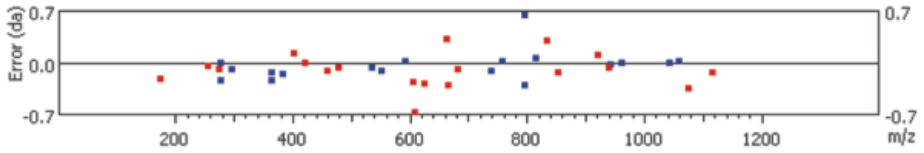

#	b	b-H2O	b-NH3	b (2+)	Seq	y	y-H2O	y-NH3	y (2+)	#
1	171.04	153.10	154.20	86.06	K(+42.01)					6
2	270.16	252.17	253.20	135.59	V	577.42	559.19	560.32	289.17	5
3	417.29	399.41	400.22	209.13	F	478.36	460.34	461.25	239.64	4
4	516.29	498.42	499.29	258.66	V	331.22	313.29	314.05	166.10	3
5	573.31	555.33	556.31	287.17	G	232.28	214.09	215.16	116.57	2
6					R	175.15	157.06	158.13	88.06	1

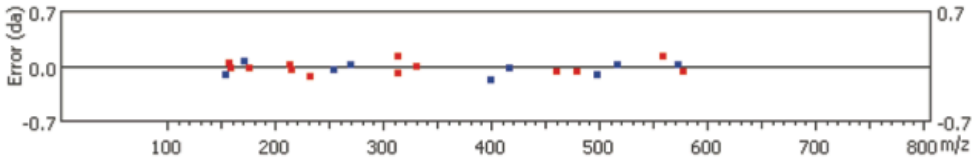

Supplementary Figure 2: Ion scores from acetylated Lys-145 and Lys-192 peptides identified from mass spectrometry analysis

(a-b) Acetylated peptides were identified by mass spectrometry analysis from immunoprecipitated TDP-43-ΔNLS protein. Listed in the table are the ion scores that correspond to the m/z spectrums obtained. The numbers listed in red bold illustrate statistical significance and the presence of acetylation at Lys-145 (a) andLys-192 (b). Mass spectrometry data were acquired with Xcaliber software (Thermo Fisher) and analyzed using PEAKS 6.0 (Bioinformatics Solutions Inc.) and Scaffold 3 software systems.

Supplementary Figure 5, Cohen *et al.*

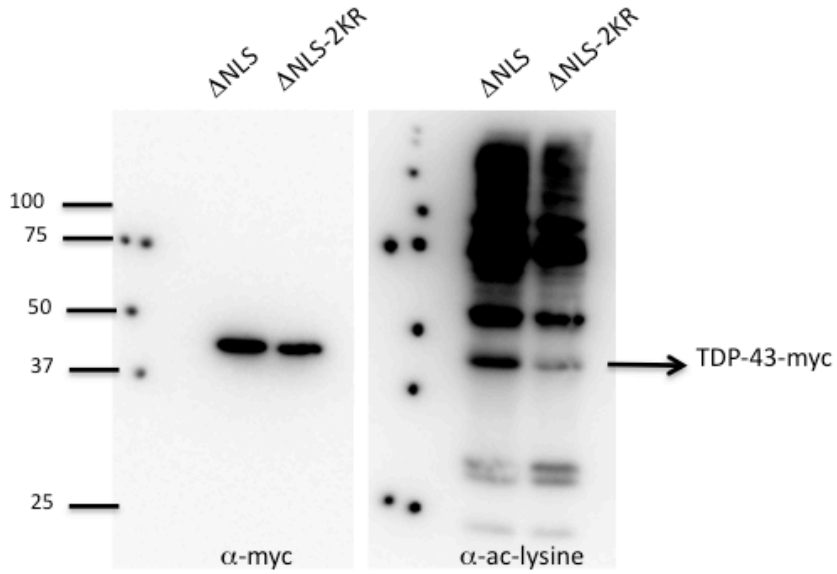

Supplementary Figure 6, Cohen *et al.*

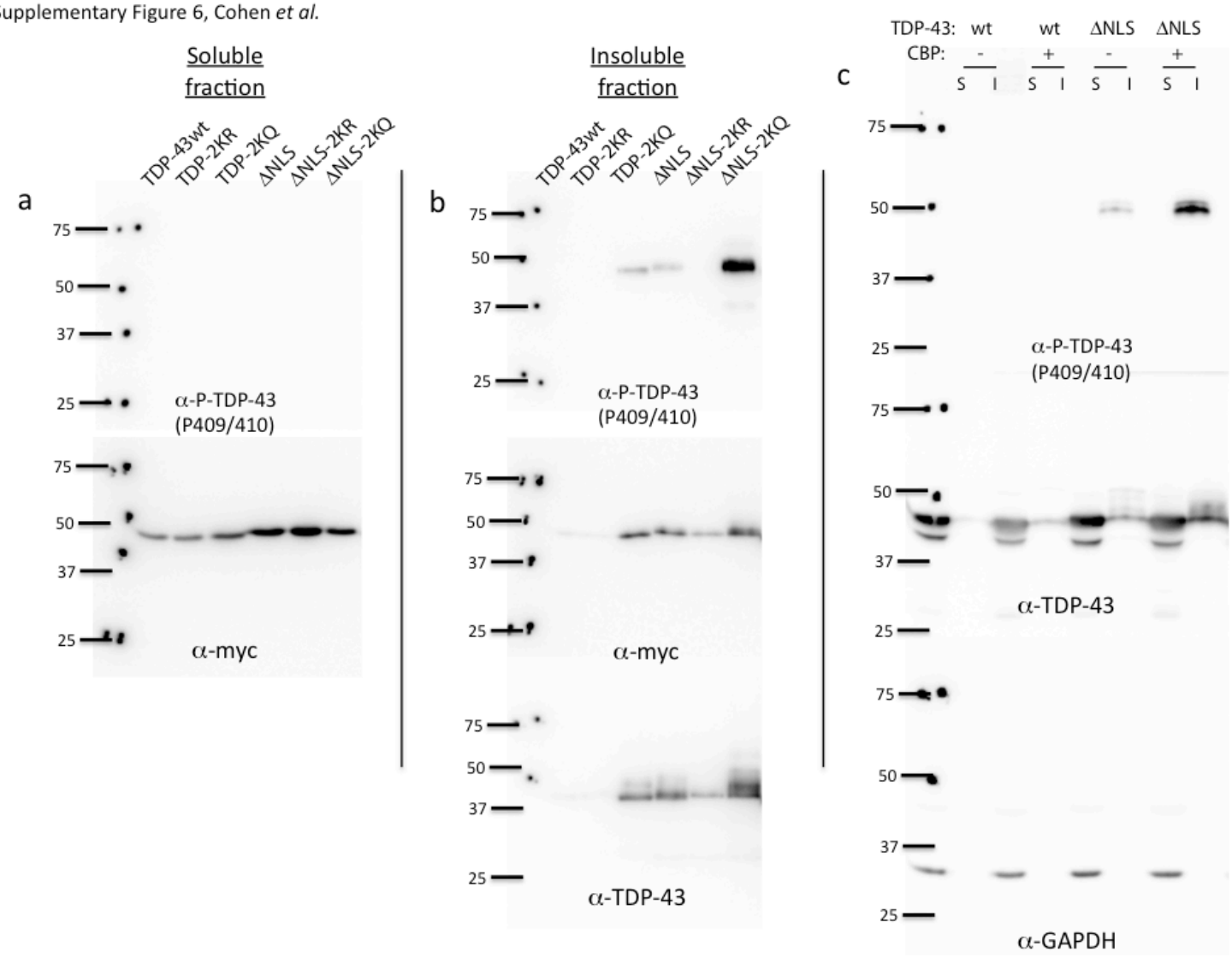

Supplementary Figure 7, Cohen *et al.*

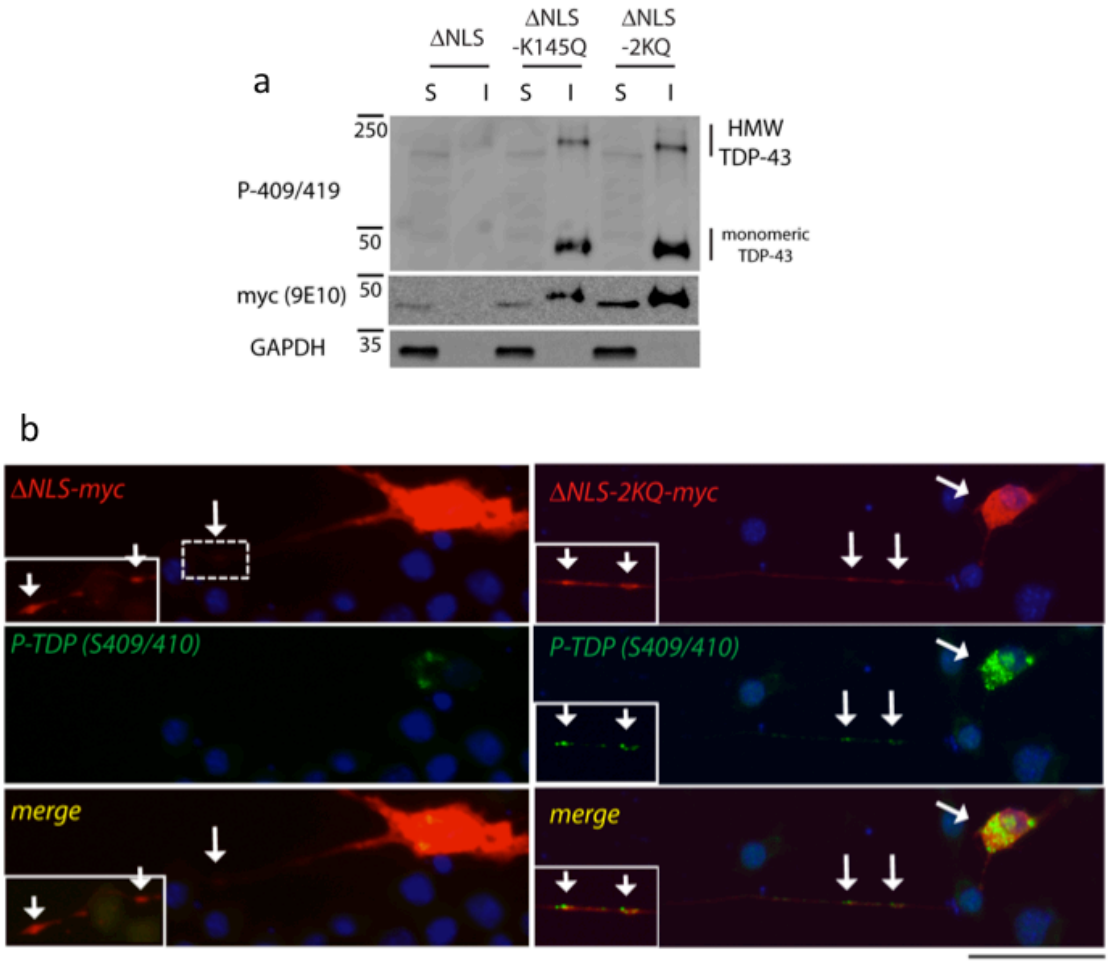

Supplementary Figure 7: TDP-43 acetylation-mimics promote TDP-43 aggregation in differentiated Neuro2A cells

Neuro2A cells were transfected with cytoplasmic TDP-43 (TDP-43-ΔNLS), or plasmids containing acetylation mimic mutations (TDP-43-ΔNLS-K145Q or TDP-43-ΔNLS-K145/192Q) for 48 hrs followed by differentiation by serum deprivation for an additional 24 hrs to extend neuritic processes. Soluble (S) and insoluble (I) cell lysates were analyzed by immunoblotting using P-409/410, myc (9E10), and GAPDH antibodies. b) Differentiated Neuro2A cells expressing non-acetylated TDP-43 (left panel) showed limited P-409/410 immunoreactivity within neurites (dashed box region is shown at higher exposure within inset to avoid image over-exposure). In contrast, the acetylation-mimic mutants (right panel), displayed strong accumulation of P-409/410-positive TDP-43 aggregates near the cell soma and distally within neurites. See white arrows highlighting transfected cells containing myc-positive TDP-43 aggregates in both soma and neurites.

Supplementary Figure 8, Cohen *et al.*

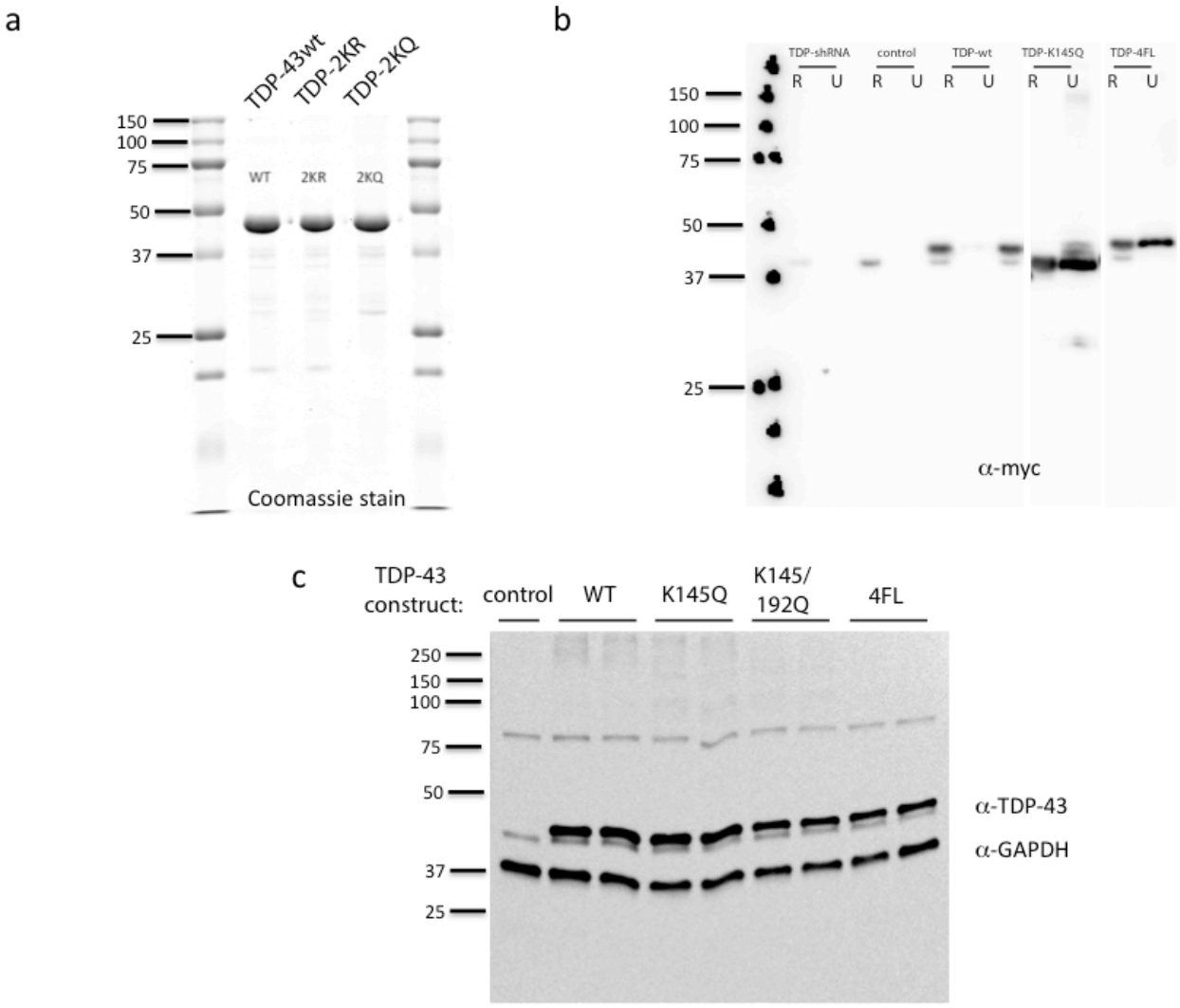

Supplementary Figure 9, Cohen *et al.*

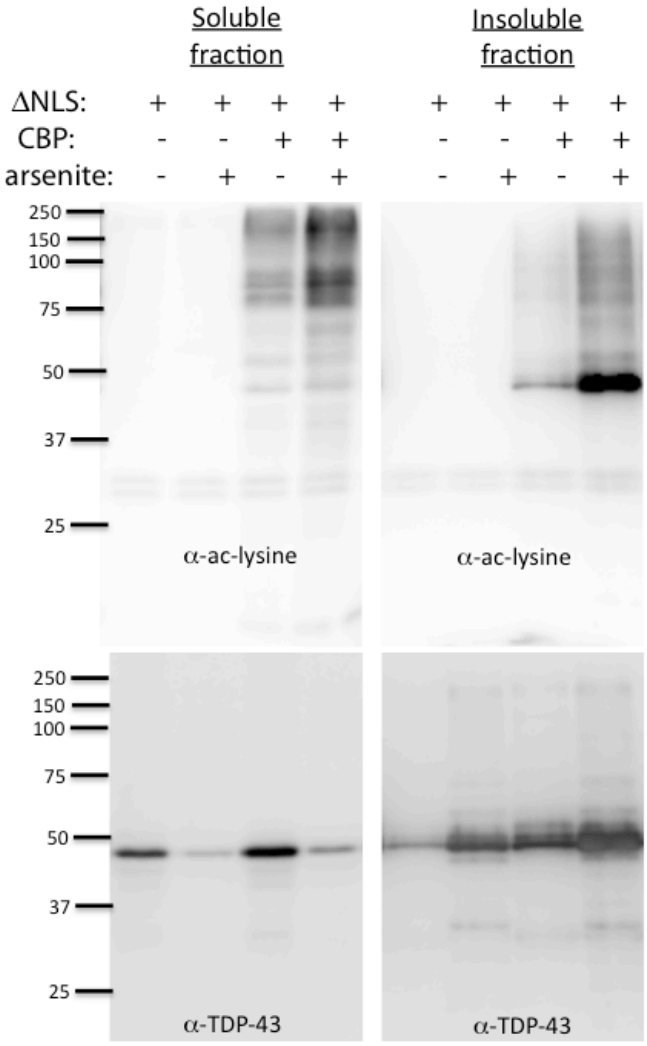

Supplementary Figure 10, Cohen *et al.*

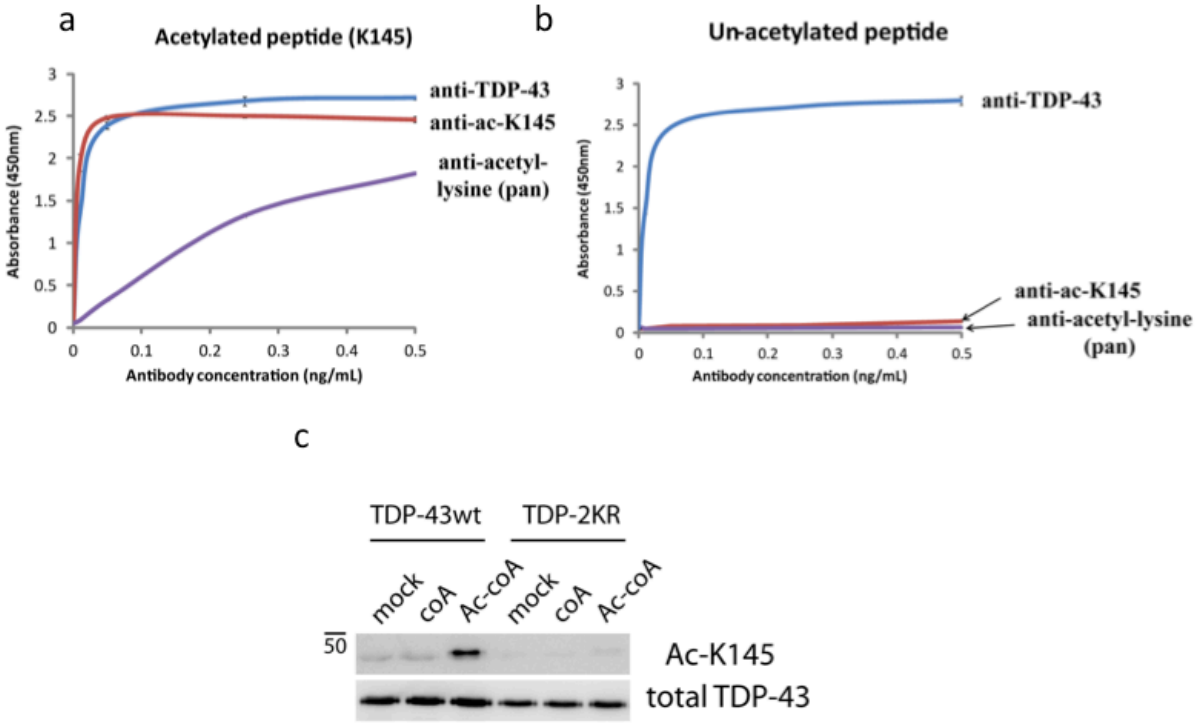

Supplementary Figure 10: Characterization of an acetylated TDP-43 antibody (Ac-K145)

a-b) ELISA assays were performed with the indicated antibodies against chemically acetylated (a) or unmodified (b) Lys-145-containing peptides consisting of the following amino acid sequence: TGHSKGFGFVR. Shown is a representative ELISA assay from N=3 independent biological replicates, and error bars represent standard deviation (SD) among triplicate experimental samples. As shown, anti-acetyl-lysine and acetylated TDP-43 antibody (Ac-K145) specifically detected the Lys-K145 acetylated peptide, but not the unmodified peptide, indicating a site-specific acetylated TDP-43 antibody. c) Recombinant WT TDP-43 or TDP-2KR (K145/192R) proteins were incubated in an acetylation reaction lacking cofactor (mock), or containing 0.4 mM coenzyme A (coA) or acetyl coenzyme A (Ac-coA) in the presence of 0.5 µg recombinant CBP for 1 hr at 37° followed by immunoblotting with Ac-K145. Acetylated WT TDP-43 protein was specifically detected by Ac-K145, while the TDP-2KR mutant protein showed diminished CBP-mediated acetylation.

Supplementary Figure 11, Cohen *et al.*

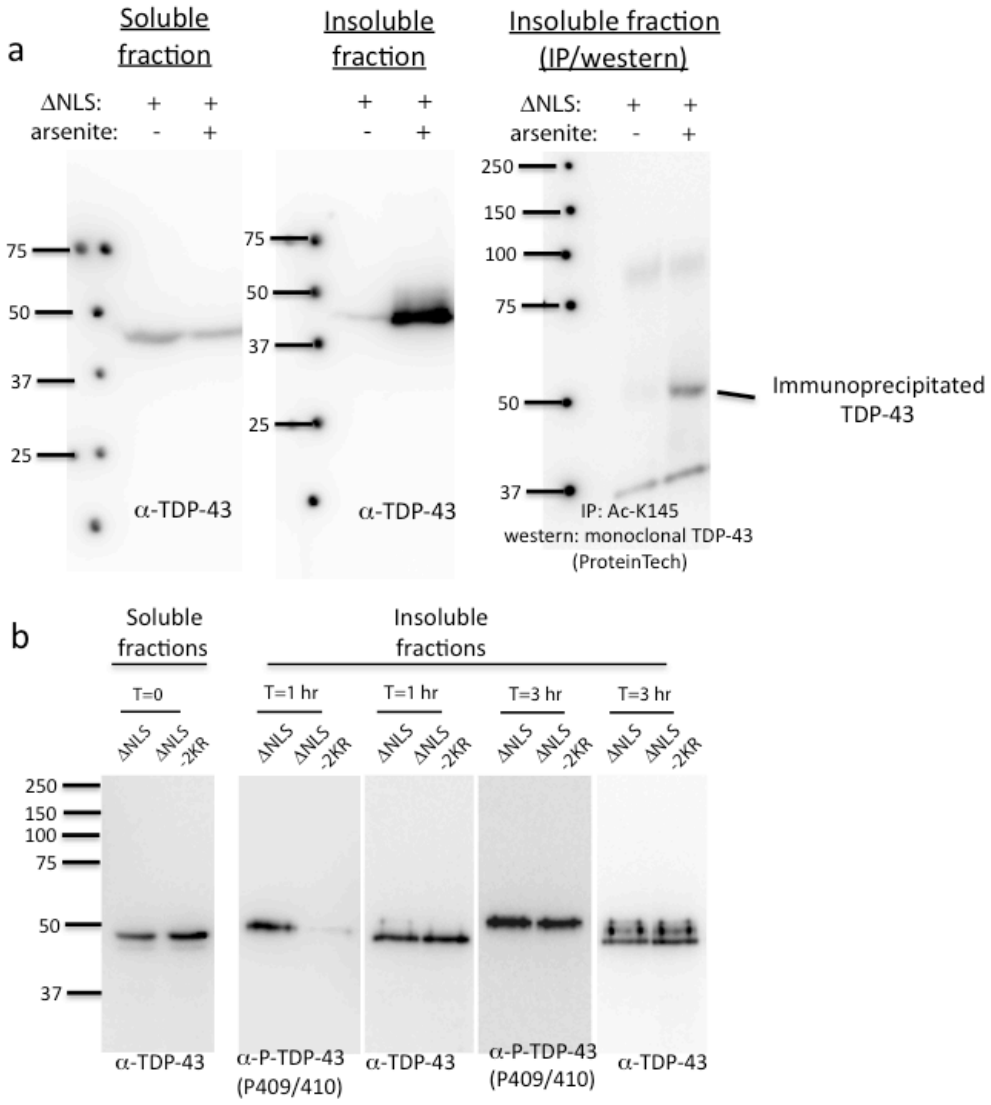

Supplementary Figure 12, Cohen *et al.*

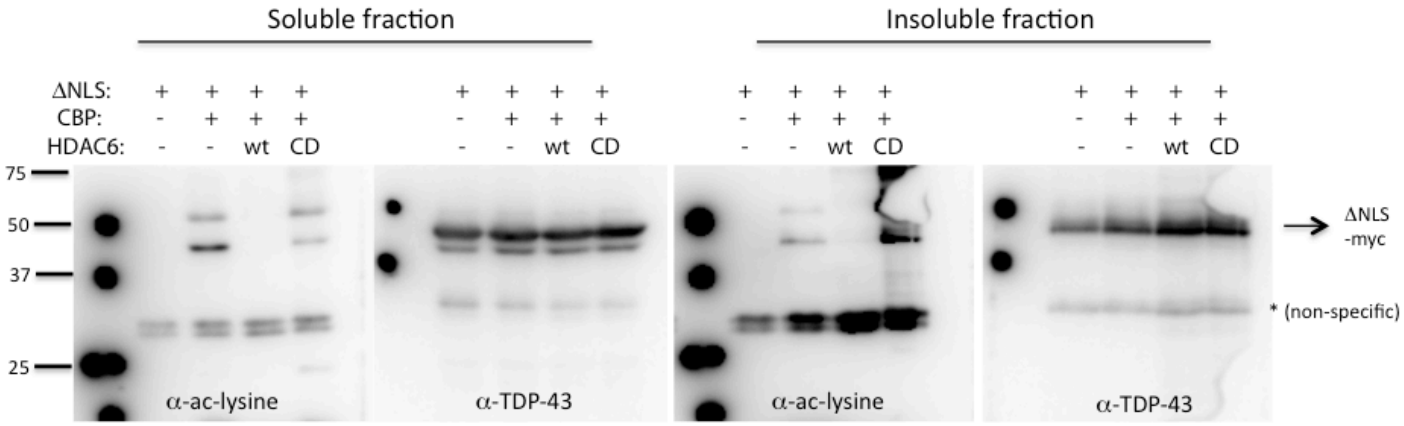

Supplementary Figure 13, Cohen *et al.*

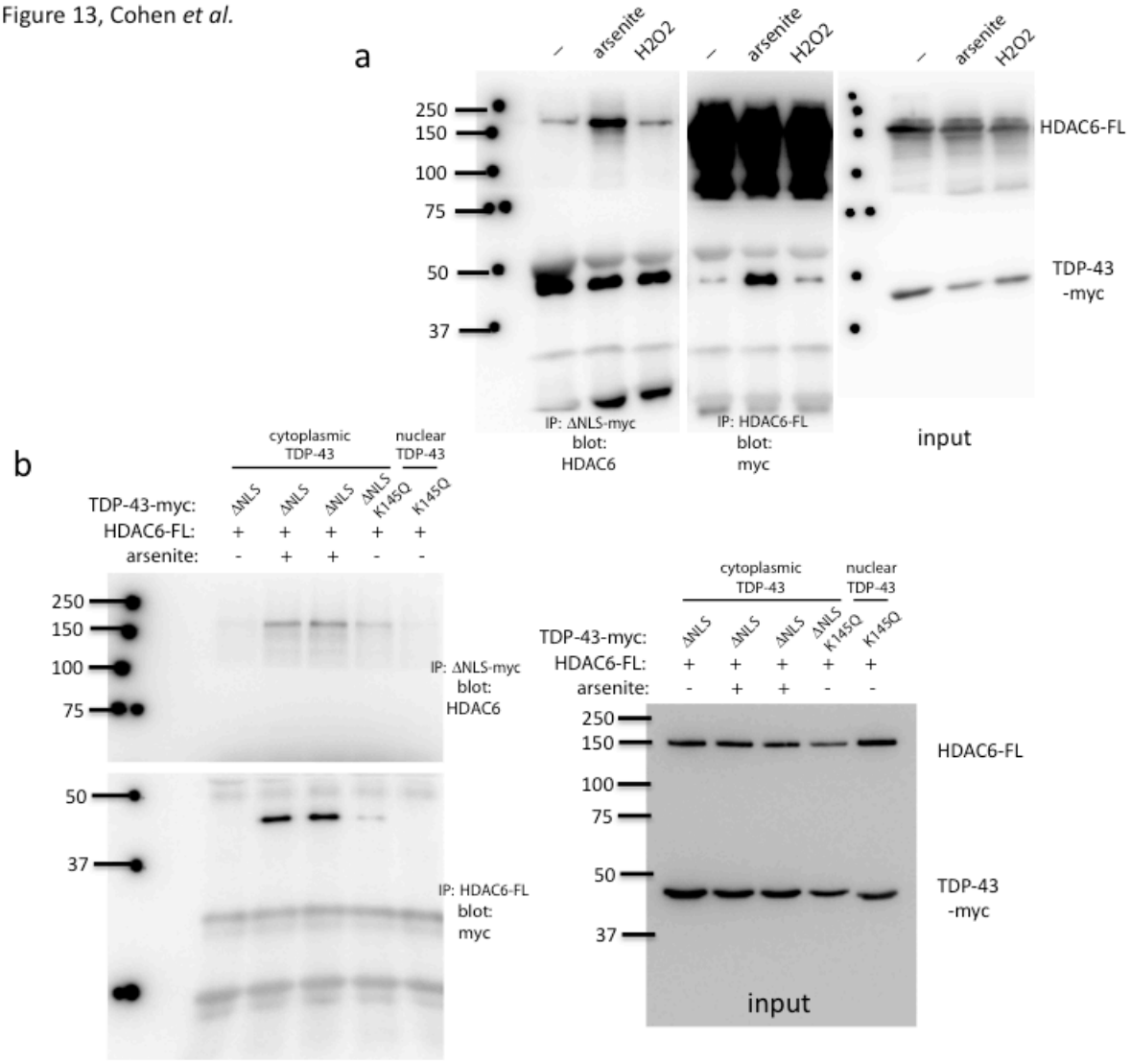

Supplementary Figure 14, Cohen *et al.*

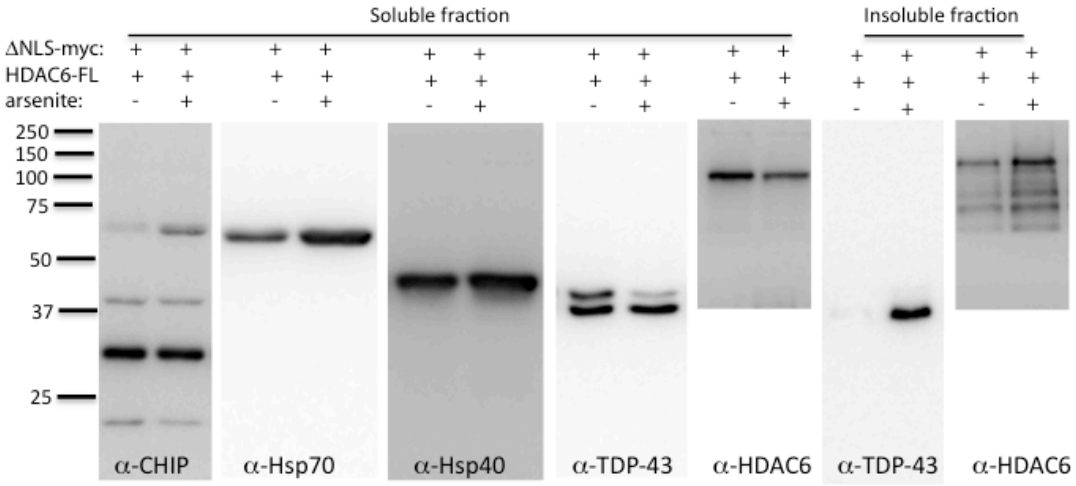

Supplementary Figure 15, Cohen *et al.*

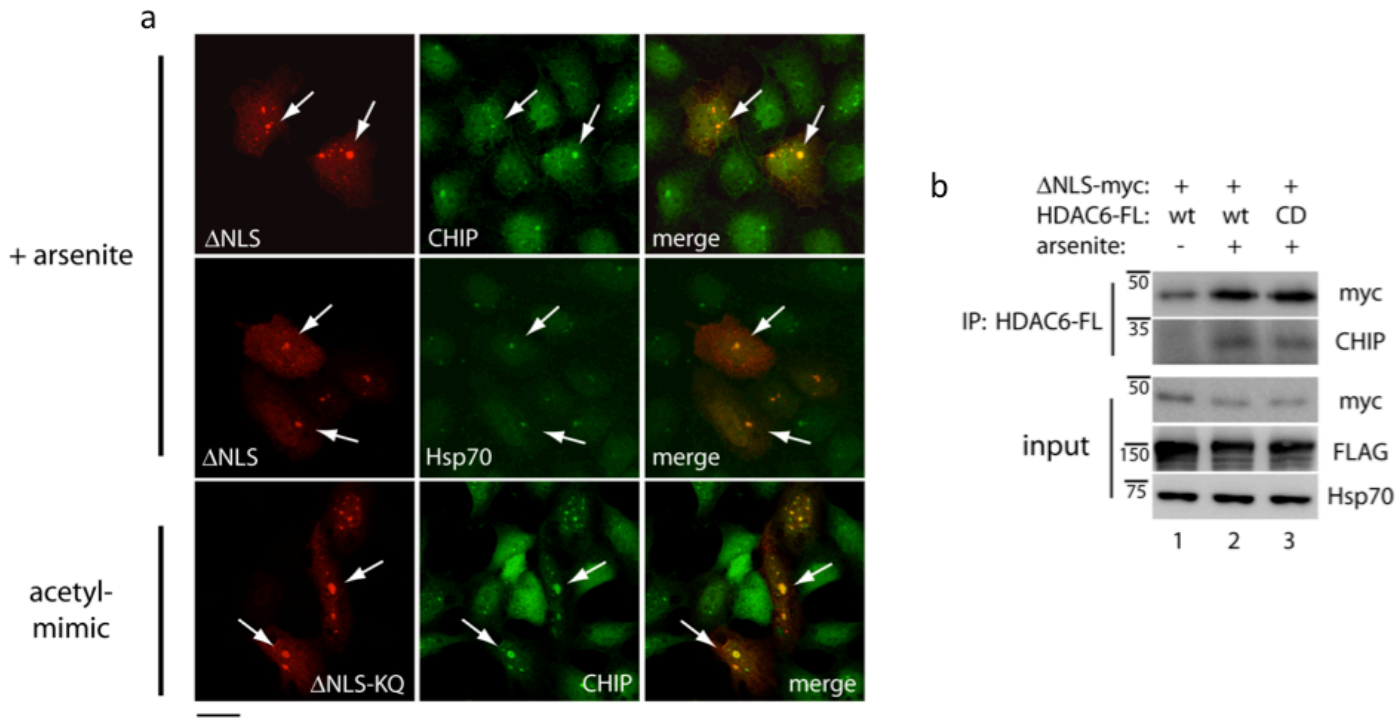

Supplementary Figure 15: Acetylated TDP-43 aggregates recruit the CHIP/Hsp70 complex

a) Double-labeling immunofluorescence microscopy illustrates that TDP-43 aggregates induced by either exposure to 0.2 mM arsenite for 1 hr (top rows) or acetylation-mimic mutations in the absence of stress (TDP-43-ΔNLS-K145Q, bottom row) are sufficient to recruit both CHIP and Hsp70 to cytoplasmic TDP-43 aggregated foci (see merged panels). Scale bar represents 25 μm. b) HDAC6-FLAG was immunoprecipitated followed by detection of myc-tagged cytoplasmic TDP-43 (TDP-43-ΔNLS) or endogenous CHIP, indicating an arsenite-inducible interaction between HDAC6 and TDP-43 that is independent of HDAC6 catalytic activity (compare lanes 2 and 3) (CD=catalytically-dead).

Supplementary Figure 16, Cohen *et al.*